

Towards Communication-efficient Federated Learning via Sparse and Aligned Adaptive Optimization

Xiumei Deng, Jun Li, Kang Wei, Long Shi, Zeihui Xiong, Ming Ding, Wen Chen, Shi Jin, and H. Vincent Poor

Abstract—Adaptive moment estimation (Adam), as a Stochastic Gradient Descent (SGD) variant, has gained widespread popularity in federated learning (FL) due to its fast convergence. However, federated Adam (FedAdam) algorithms suffer from a threefold increase in uplink communication overhead compared to federated SGD (FedSGD) algorithms, which arises from the necessity to transmit both local model updates and first and second moment estimates from distributed devices to the centralized server for aggregation. Driven by this issue, we propose a novel sparse FedAdam algorithm called FedAdam-SSM, wherein distributed devices sparsify the updates of local model parameters and moment estimates and subsequently upload the sparse representations to the centralized server. To further reduce the communication overhead, the updates of local model parameters and moment estimates incorporate a shared sparse mask (SSM) into the sparsification process, eliminating the need for three separate sparse masks. Theoretically, we develop an upper bound on the divergence between the local model trained by FedAdam-SSM and the desired model trained by centralized Adam, which is related to sparsification error and imbalanced data distribution. By minimizing the divergence bound between the model trained by FedAdam-SSM and centralized Adam, we optimize the SSM to mitigate the learning performance degradation caused by sparsification error. Additionally, we provide convergence bounds for FedAdam-SSM in both convex and non-convex objective function settings, and investigate the impact of local epoch, learning rate and sparsification ratio on the convergence rate of FedAdam-SSM. Experimental results show that FedAdam-SSM outperforms baselines in terms of convergence rate (over 1.1× faster than the sparse FedAdam baselines) and test accuracy (over 14.5% ahead of the quantized FedAdam baselines).

Index Terms—Federated Learning, Adam Optimizer, Sparsification method.

I. INTRODUCTION

X. Deng, J. Li and L. Shi are with School of Electronic and Optical Engineering, Nanjing University of Science and Technology, Nanjing 210094, China (e-mail: {xiumeideng, jun.li}@njjust.edu.cn; slong1007@gmail.com).

K. Wei is with the Department of Computing, Hong Kong Polytechnic University, Hong Kong 999077, China (e-mail: kangwei@polyu.edu.hk).

Z. Xiong is with the Pillar of Information Systems Technology and Design, Singapore University of Technology and Design, Singapore (e-mail: zehui_xiong@sutd.edu.sg).

M. Ding is with Data61, CSIRO, Sydney, NSW 2015, Australia (e-mail: ming.ding@data61.csiro.au).

W. Chen is with Department of Electronics Engineering, Shanghai Jiao Tong University, Shanghai 200240, China (e-mail: wenchen@sjtu.edu.cn).

S. Jin is with the National Mobile Communications Research Laboratory, Southeast University, Nanjing 210096, China (e-mail: jinshi@seu.edu.cn).

H. V. Poor is with Department of Electrical and Computer Engineering, Princeton University, NJ 08544, USA (e-mail: poor@princeton.edu).

RECENT advances in Internet of Things (IoT) and Artificial Intelligence (AI) technologies have empowered next-generation smart devices to bring us higher levels of comfort, convenience, connectivity, and intelligence [1]–[3]. The explosion of IoT data, limited data transmission capacity, as well as potential data privacy and security threats, make it impractical to upload all the raw data to a remote cloud for centralized machine learning (ML) [4], [5]. To avoid collecting private data from distributed devices, federated learning (FL) has emerged as a privacy-enhancing distributed ML paradigm [6]–[8], where distributed devices perform local model training on their private datasets, and a centralized server aggregates the uploaded local models to build a global model.

In recent years, the size of ML models has dramatically increased to achieve high accuracy and adapt to dynamic environments in many application scenarios such as computer vision, natural language processing and speech recognition [9], [10]. In practice, ML models, especially deep learning models, are typically hundreds of megabytes or even gigabytes in size. As the size of state-of-the-art ML models continues to explode, the implementation of an efficient FL paradigm faces the following challenges. 1) *Convergence speed*. Stochastic Gradient Descent (SGD) has been widely applied to FL training. Despite its simplicity, the vanilla SGD suffers from slow convergence, and is sensitive to variations in hyperparameters (e.g., learning rate). To reduce the computational burden on distributed devices throughout the FL training process, it is paramount to deploy advanced optimizers to improve the convergence rate while maintaining model accuracy. 2) *Communication overhead*. Since distributed devices in FL frequently upload/download ML models to/from the centralized server, large-scale ML models inevitably lead to unaffordable communication overhead. Especially in wireless networks, high traffic between distributed devices and the centralized server can overwhelm the limited transmission bandwidth, resulting in frequent interruptions, prolonged latencies and prohibitive costs.

As a variant of SGD, adaptive moment estimation (Adam) has gained widespread popularity in FL due to its fast convergence and intuitive explanations behind the adaptive hyperparameters [11], [12]. However, federated Adam (FedAdam for short) algorithms suffer from a threefold increase in uplink communication overhead compared to federated SGD (FedSGD for short) algorithms, which arises from the necessity to transmit both local model updates and first and second

moment estimates (i.e., exponential moving averages of historical gradients and gradient squares) from distributed devices to the centralized server for aggregation. Despite current efforts to enhance the convergence rate of FedAdam algorithms, how to reduce this communication overhead remains open in the literature. Driven by this issue, we propose a novel sparsification method for communication-efficient FedAdam. The main contributions of this paper are summarized as follows:

- 1) **FedAdam-SSM.** We propose a sparse FedAdam algorithm called FedAdam-SSM, wherein distributed devices sparsify the updates of local model parameters and moment estimates and subsequently upload the sparse representations to the centralized server. To further reduce the communication overhead, the updates of local model parameters and moment estimates incorporate a shared sparse mask (SSM) into the sparsification process, eliminating the need for three separate sparse masks. Compared with the standard FedAdam, FedAdam-SSM effectively reduces the uplink communication overhead from $O(3dq)$ to $O(3kq + d)$.
- 2) **Shared sparse mask design.** We optimize the SSM to mitigate the learning performance degradation caused by the sparsification error. Firstly, we provide an upper bound on the divergence between the local model trained by FedAdam-SSM and the desired model trained by centralized Adam. To minimize the sparsification error of FedAdam-SSM, we devise an optimal SSM by minimizing the divergence bound between FedAdam-SSM and centralized Adam.
- 3) **Convergence analysis.** We provide convergence bounds for FedAdam-SSM in both non-convex and convex objective function settings. We prove that the convergence rate of FedAdam-SSM achieves a linear speedup of $O(\frac{1}{\sqrt{T}})$ in the non-convex setting, and can be further increased to $O(\frac{1}{T})$ in the convex setting. Additionally, we investigate the impact of local epoch, learning rate and sparsification ratio on the convergence rate of FedAdam-SSM, and provides guidance for selecting appropriate values of local epoch and learning rate to improve the learning performance of FedAdam-SSM.
- 4) **Experimental results.** We conduct extensive experiments involving training of Convolutional Neural Network (CNN), Visual Geometry Group-11 (VGG-11) and Residual Network-18 (ResNet-18) over Fashion-MNIST, CIFAR-10 and SVHN datasets to investigate the training performance of the proposed FedAdam-SSM. The experimental results verify our theoretical analysis and show that FedAdam-SSM outperforms baselines in terms of convergence rate (over $1.1\times$ faster than the best sparse FedAdam baseline) and test accuracy (over 14.5% ahead of the best quantized FedAdam baseline).

The remainder of this paper is organized as follows. Section II discusses related works. Section III briefly provides some background on FL, FedAdam and the sparsification methods. In Section IV, we propose the FedAdam-SSM algorithm. In Section V, we optimize the SSM to mitigate the sparsification error. Section VI conducts the convergence analysis, and

Section VII represents the experimental results. Section VIII concludes this paper.

II. SIGNIFICANCE AND RELATED WORK

In this section, we review two lines of work that are most related to this paper, i.e., SGD variants in FL and communication-efficient FL.

A. SGD variants in FL

The low convergence rate and the considerable effort required to find the optimal hyper-parameters of vanilla SGD can place a significant burden on the computational capacity of distributed devices, leading to long FL training sessions and unsatisfactory quality of experience. To accelerate the model convergence, recent works have developed a variety of SGD variants in the FL setting. The authors in [13] and [14] propose a Nesterov Accelerated Gradient Descent (NAG) based FL framework named FedNAG to speed up FL convergence, where distributed devices locally update the model parameters and first momentum estimates, and upload the local model parameters and momentum estimates to the centralized server for aggregation. The convergence analysis presented in [13] reveals that FedNAG can converge faster than FedSGD. Using the variance-reduced SGD (SVRG) optimizer, the works in [15] and [16] improve the FL convergence rate by gradually eliminating the inherent variance of the gradients. Later on, by adaptively tuning the learning rate with both the first momentum estimate and the second momentum estimate, the works in [17]–[19] develop different FedAdam algorithms to accelerate the training process, and prove the convergence of the proposed algorithms for both convex and non-convex settings.

From the above, the integration of SGD variants into FL has proven to improve the convergence rate in the training process, especially for Adam. FedAdam algorithms not only have well-documented empirical performance, but can also be shown theoretically to escape saddle points and converge to second-order stationary points faster than FedSGD. On the one hand, FedAdam accelerates the FL convergence thanks to the adaptive learning rate tuned by the first and second momentum estimates. On the other hand, the first and second momentum estimates have to be uploaded to the centralized server for aggregation, which significantly increases the uplink communication overhead. To this end, strategies to reduce the communication overhead are of considerable importance in improving the training efficiency of FedAdam.

B. Communication-efficient Federated Learning

In order to achieve communication-efficient FL, different methods to reduce the communication overhead have been proposed in the literature. Early works have considered device scheduling and communication resource allocation. The authors in [20] and [21] optimize the device selection as well as communication and computational resource allocation to minimize the training latency while guaranteeing FL performance. However, when dealing with large-scale ML models

and limited communication resources, device scheduling and communication resource allocation alone to reduce communication overhead may prove insufficient in achieving the desired training efficiency.

More recently, compression techniques such as quantization and sparsification methods have been introduced into FL to reduce the size of local model updates transmitted to the centralized server. The authors in [22]–[26] develop different quantization or sparsification strategies, which adaptively tune the quantization level or sparsification ratio to reduce the communication overhead while guaranteeing a low compression error. Going forward, the implementation of compression methods in FedAdam algorithms remains challenging. The authors in [27] and [28] propose two different communication-efficient FedAdam algorithms, which quantize local model updates or model parameters to reduce the communication cost, and compensate for the quantization errors using an error-feedback technique. To further improve the model accuracy, [29] proposes a 2-phase FedAdam algorithm, which runs the standard FedAdam in the warm-up phase, and computes the second moment estimates as a fixed precondition for the quantized FedAdam in the compression phase.

However, the works in [27]–[29] set the number of local epochs to 1, which results in extremely frequent communication between distributed devices and the centralized server and thereby increases both the compression error and the communication overhead in FedAdam. Moreover, these works fail to consider the aggregation of the first and second local momentum estimates to obtain global momentum estimates in each communication round, which results in the utilization of out-of-date momentum estimates in the training process and consequently causes a degradation in FL performance. Subsequently, [30] adopts two different quantization methods (i.e., uniform and exponential quantization methods) to quantize the local model updates and the momentum estimates in the proposed FedAdam algorithm. However, due to the fact that Adam depends non-linearly on the gradient, the authors do not provide a convergence analysis of quantized FedAdam.

In our work, we integrate the sparsification method with the standard FedAdam. Different from the aforementioned works on communication-efficient FedAdam [28]–[30], we take into account the up-to-date global momentum estimates by sparsifying the updates of local model parameters and momentum estimates before uploading them to the centralized server in each communication round. To further alleviate the communication overhead, we incorporate a shared sparse mask into the sparsification of the updates of local model parameters and moment estimates. To mitigate the learning performance degradation caused by the sparsification error, we optimize the shared sparse mask by minimizing the divergence bound between the local model trained by FedAdam-SSM and the desired model trained by centralized Adam. To the best of our knowledge, our work represents the first attempt to design a shared sparse mask for the sparsification of the updates of local model parameters and moment estimates in sparse FedAdam and to provide a theoretical analysis of this approach.

III. PRELIMINARIES AND BACKGROUND

In this section, we overview a few important concepts and definitions with regard to FedAdam and sparsification method.

A. FedAdam

Consider an FL network of N devices collaborating to train an ML model over their respective local datasets. Let $\mathcal{N} = \{1, 2, \dots, N\}$ denote the index set of the devices. The goal of FL is to find a set of model parameters $\mathbf{w}^* \in \mathbb{R}^d$ that minimizes the global loss function $F(\mathbf{w})$ on all the local datasets, i.e.,

$$F(\mathbf{w}) = \frac{\sum_{n=1}^N |\mathcal{D}_n| f(\mathbf{w}, \mathcal{D}_n)}{\sum_{n=1}^N |\mathcal{D}_n|}, \quad (1)$$

where $f(\mathbf{w}, \mathcal{D}_n)$ denotes the loss function on the local dataset \mathcal{D}_n . In standard FedSGD, distributed devices utilize SGD to minimize the local loss function $F_n(\mathbf{w})$ on its local dataset by updating the local model parameters over a total of L local epochs. The update rule in the l -th local epoch is

$$\mathbf{w}_n^{l+1,t} = \mathbf{w}_n^{l,t} - \eta \nabla f(\mathbf{w}_n^{l,t}, \tilde{\mathcal{D}}_n), \quad (2)$$

where $\mathbf{w}_n^{l,t}$ denotes the local model parameters of the n -th device in the l -th local epoch and t -th communication round, $\eta > 0$ is the learning rate, $\nabla f(\mathbf{w}_n^{l,t}, \tilde{\mathcal{D}}_n)$ is the mini-batch stochastic gradient of the local loss function, and $\tilde{\mathcal{D}}_n$ is a batch of the local dataset \mathcal{D}_n .

To improve the accuracy of the ML model and accelerate the training process, Adam was proposed as a variant of SGD by taking into consideration momentum and root mean square propagation [27]–[29]. To be specific, it takes advantage of momentum by moving in the negative direction of the first moment estimate of the gradient, and maintains a per-parameter learning rate adjusted to the second moment estimate of the gradient. Using Adam, the local model update rule in FL training can be written as

$$\mathbf{w}_n^{l,t} = \mathbf{w}_n^{l-1,t} - \eta \frac{\mathbf{m}_n^{l,t}}{\sqrt{\mathbf{v}_n^{l,t} + \epsilon}}, \quad (3)$$

where $\mathbf{m}_n^{l,t}$ and $\mathbf{v}_n^{l,t}$ are the first and second moment estimates of the gradient, and ϵ is a safety offset for division by the second moment estimate. Specifically, the first and second moment estimates $\mathbf{m}_n^{l,t}$ and $\mathbf{v}_n^{l,t}$ are computed as

$$\mathbf{m}_n^{l,t} = \beta_1 \mathbf{m}_n^{l-1,t} + (1 - \beta_1) \nabla f(\mathbf{w}_n^{l-1,t}, \tilde{\mathcal{D}}_n), \quad (4)$$

$$\mathbf{v}_n^{l,t} = \beta_2 \mathbf{v}_n^{l-1,t} + (1 - \beta_2) \left(\nabla f(\mathbf{w}_n^{l-1,t}, \tilde{\mathcal{D}}_n) \right)^2, \quad (5)$$

where $\beta_1 \in [0, 1)$ and $\beta_2 \in [0, 1)$ control the exponential decay rates of the moving averages. Therefore, the procedure of FedAdam in each communication round is as follows:

- 1) According to the update rule in (3), (4), and (5), each device updates the local moment estimates and model parameters (i.e., $\mathbf{m}_n^{l,t}$, $\mathbf{v}_n^{l,t}$, and $\mathbf{w}_n^{l,t}$) over a total of L local epochs at the beginning of each round.
- 2) Each device uploads the updated local moment estimates and model parameters (i.e., $\mathbf{m}_n^{L,t}$, $\mathbf{v}_n^{L,t}$, and $\mathbf{w}_n^{L,t}$) to the centralized server.

Algorithm 1: FedAdam

```

1 Initialize:  $\mathbf{W}^0, \mathbf{M}^0 \leftarrow 0, \mathbf{V}^0 \leftarrow 0$ ;
2 for each communication round  $t = 0, 1, \dots, T - 1$  do
3   do in parallel
4     for each device  $n = 1, 2, \dots, N$  do
5       Download  $\mathbf{M}^t, \mathbf{V}^t, \mathbf{W}^t$  from the server;
6       Set  $\mathbf{w}_n^{0,t} \leftarrow \mathbf{W}^t, \mathbf{m}_n^{0,t} \leftarrow \mathbf{M}^t, \mathbf{v}_n^{0,t} \leftarrow \mathbf{V}^t$ ;
7       Update  $\mathbf{m}_n^{l,t}, \mathbf{v}_n^{l,t}$ , and  $\mathbf{w}_n^{l,t}$  according to (4),
          (5), and (3) over  $L$  local epochs;
8       Upload  $\mathbf{m}_n^{L,t}, \mathbf{v}_n^{L,t}$ , and  $\mathbf{w}_n^{L,t}$  to the server;
9   The server updates  $\mathbf{M}^{t+1}, \mathbf{V}^{t+1}, \mathbf{W}^{t+1}$  according to
      FedAvg;
    
```

- 3) Upon receiving all the local moment estimates and local model parameters, the centralized server updates the global moment estimates and model parameters according to the federated averaging (FedAvg) algorithm, i.e., $\mathbf{M}^{t+1} = \frac{\sum_{n=1}^N |\mathcal{D}_n| \mathbf{m}_n^{L,t}}{\sum_{n=1}^N |\mathcal{D}_n|}$, $\mathbf{V}^{t+1} = \frac{\sum_{n=1}^N |\mathcal{D}_n| \mathbf{v}_n^{L,t}}{\sum_{n=1}^N |\mathcal{D}_n|}$, and $\mathbf{W}^{t+1} = \frac{\sum_{n=1}^N |\mathcal{D}_n| \mathbf{w}_n^{L,t}}{\sum_{n=1}^N |\mathcal{D}_n|}$.
- 4) Each device downloads the updated global moment estimates and model parameters from the centralized server for the next communication round of FedAdam.

B. Sparsification Method

To reduce the communication overhead, sparsification methods have been extensively studied in FL to convert the local model parameters or accumulated gradients into a sparse representation before they are transmitted from distributed devices to the centralized server. Specifically, each device in FL induces a sparse mask on the d -dimensional vector to map each element of the vector to either its original value or zero, and transmit the values of the non-zero elements and the sparse mask to the centralized server. The top- k sparsifier used in this paper is defined as follows:

Definition 1: (Top- k sparsifier). For any positive integer $1 \leq k \leq d$ and any vector $\mathbf{x} \in \mathbb{R}^d$, the top- k sparsifier $\text{Top}_k: \mathbb{R}^d \rightarrow \mathbb{R}^d$ is defined as

$$\text{Top}_k(\mathbf{x}) := \mathbf{x} \odot \mathbb{1}_{\text{Top}_k}(\mathbf{x}), \quad (6)$$

where $\mathbb{1}_{\text{Top}_k}(\mathbf{x}) \in \{0, 1\}^d$ represents the sparse mask of Top_k , and \odot performs the element-wise product. The sparse mask of Top_k is defined as

$$(\mathbb{1}_{\text{Top}_k}(\mathbf{x}))_{\pi(j)} := \begin{cases} 1, & \text{if } j \leq k, \\ 0, & \text{otherwise,} \end{cases} \quad (7)$$

where π is a permutation of $[d]$ such that $|(\mathbf{x})_{\pi(j)}| \geq |(\mathbf{x})_{\pi(j+1)}|$ for $j \in [1, d-1]$.

It is clear to see that the top- k sparsifier selects the top k largest elements in terms of the absolute value. In addition, the top- k sparsifier satisfies the k -contraction property [31], [32] as follows:

Definition 2: (k -contraction property). For a positive integer $1 \leq k \leq d$ and any vector $\mathbf{x} \in \mathbb{R}^d$, a k -contraction operator $\text{Comp}: \mathbb{R}^d \rightarrow \mathbb{R}^d$ satisfies the contraction property:

$$\mathbb{E} [\|\mathbf{x} - \text{Comp}(\mathbf{x})\|^2] \leq \left(1 - \frac{k}{d}\right) \|\mathbf{x}\|^2. \quad (8)$$

Notably, the sparsification ratio is defined as the ratio of originally-valued elements over all elements, i.e.,

$$\alpha = \frac{k}{d}. \quad (9)$$

IV. FEDADAM-SSM

In this section, we first present a straightforward sparse FedAdam algorithm called FedAdam-Top, which separately sparsifies the updates of local model parameters and moment estimates with the top- k sparsifier. Building upon FedAdam-Top, we propose FedAdam-SSM, which incorporates an SSM into the sparsification of the updates of local model parameters and moment estimates to further reduce the uplink communication overhead.

Using the top- k sparsifier, FedAdam-Top carries out in a different fashion from the standard FedAdam as follows:

- 1) Let $\Delta \mathbf{M}_n^t = \mathbf{m}_n^{L,t} - \mathbf{M}^t$, $\Delta \mathbf{V}_n^t = \mathbf{v}_n^{L,t} - \mathbf{V}^t$, and $\Delta \mathbf{W}_n^t = \mathbf{w}_n^{L,t} - \mathbf{W}^t$ denote the updates of local moment estimates and model parameters. Upon completing the local model training, each device sparsifies the updates with the top- k sparsifier, i.e., $\Delta \hat{\mathbf{M}}_n^t = \Delta \mathbf{M}_n^t \odot \mathbb{1}_{\text{Top}_k}(\Delta \mathbf{M}_n^t)$, $\Delta \hat{\mathbf{V}}_n^t = \Delta \mathbf{V}_n^t \odot \mathbb{1}_{\text{Top}_k}(\Delta \mathbf{V}_n^t)$, and $\Delta \hat{\mathbf{W}}_n^t = \Delta \mathbf{W}_n^t \odot \mathbb{1}_{\text{Top}_k}(\Delta \mathbf{W}_n^t)$. Then, each device uploads the top- k sparse masks (i.e., $\mathbb{1}_{\text{Top}_k}(\Delta \mathbf{M}_n^t)$, $\mathbb{1}_{\text{Top}_k}(\Delta \mathbf{V}_n^t)$, and $\mathbb{1}_{\text{Top}_k}(\Delta \mathbf{W}_n^t)$) and the values of the non-zero elements of the sparse vectors (i.e., $\Delta \hat{\mathbf{M}}_n^t$, $\Delta \hat{\mathbf{V}}_n^t$, and $\Delta \hat{\mathbf{W}}_n^t$) to the centralized server.
- 2) The centralized server reconstructs the sparse vectors $\Delta \hat{\mathbf{M}}_n^t$, $\Delta \hat{\mathbf{V}}_n^t$, and $\Delta \hat{\mathbf{W}}_n^t$ using the received sparse masks and values of the non-zero elements, and computes the updates of global moment estimates and model parameters as $\Delta \hat{\mathbf{M}}^t = \frac{\sum_{n=1}^N |\mathcal{D}_n| \Delta \hat{\mathbf{M}}_n^t}{\sum_{n=1}^N |\mathcal{D}_n|}$, $\Delta \hat{\mathbf{V}}^t = \frac{\sum_{n=1}^N |\mathcal{D}_n| \Delta \hat{\mathbf{V}}_n^t}{\sum_{n=1}^N |\mathcal{D}_n|}$, and $\Delta \hat{\mathbf{W}}^t = \frac{\sum_{n=1}^N |\mathcal{D}_n| \Delta \hat{\mathbf{W}}_n^t}{\sum_{n=1}^N |\mathcal{D}_n|}$. Afterwards, the centralized server transmits the updates of global moment estimates and model parameters $\Delta \hat{\mathbf{M}}^t$, $\Delta \hat{\mathbf{V}}^t$, and $\Delta \hat{\mathbf{W}}^t$ to each device.
- 3) Upon receiving $\Delta \hat{\mathbf{M}}^t$, $\Delta \hat{\mathbf{V}}^t$, and $\Delta \hat{\mathbf{W}}^t$, each device updates the global moment estimates and model parameters as follows: $\mathbf{M}^{t+1} = \mathbf{M}^t + \Delta \hat{\mathbf{M}}^t$, $\mathbf{V}^{t+1} = \mathbf{V}^t + \Delta \hat{\mathbf{V}}^t$, and $\mathbf{W}^{t+1} = \mathbf{W}^t + \Delta \hat{\mathbf{W}}^t$.

It can be seen that by separately sparsifying the updates of local moment estimates and model parameters $\Delta \mathbf{M}_n^t$, $\Delta \mathbf{V}_n^t$, and $\Delta \mathbf{W}_n^t$ with the top- k sparsifier, distributed devices in FedAdam-Top transmit the values of the top k largest elements of the vectors and the top- k sparse masks to the centralized server instead of the raw vectors. Let q denote the floating-point precision. The total number of bits for uplink data transmission per communication round in FedAdam-Top is $3N(kq + d)$. Note that the total number of bits for uplink data transmission per communication round in the standard FedAdam is $3Ndq$. Therefore, the uplink data transmission volume per communication round can be reduced from

Algorithm 2: FedAdam-SSM

```

1 Initialize:  $\mathbf{W}^0, \mathbf{M}^0 \leftarrow 0, \mathbf{V}^0 \leftarrow 0, \Delta\hat{\mathbf{W}}^0 \leftarrow 0,$ 
    $\Delta\hat{\mathbf{M}}^0 \leftarrow 0, \Delta\hat{\mathbf{V}}^0 \leftarrow 0;$ 
2 for each communication round  $t = 1, \dots, T$  do
3   do in parallel
4     for each device  $n = 1, 2, \dots, N$  do
5       Download  $\Delta\hat{\mathbf{M}}^{t-1}, \Delta\hat{\mathbf{V}}^{t-1}, \Delta\hat{\mathbf{W}}^{t-1}$  from the
6         server;
7       Update  $\mathbf{M}^t \leftarrow \mathbf{M}^{t-1} + \Delta\hat{\mathbf{M}}^{t-1},$ 
8          $\mathbf{V}^t \leftarrow \mathbf{V}^{t-1} + \Delta\hat{\mathbf{V}}^{t-1},$ 
9          $\mathbf{W}^t \leftarrow \mathbf{W}^{t-1} + \Delta\hat{\mathbf{W}}^{t-1};$ 
10      Set  $\mathbf{w}_n^{0,t} \leftarrow \mathbf{W}^t, \mathbf{m}_n^{0,t} \leftarrow \mathbf{M}^t, \mathbf{v}_n^{0,t} \leftarrow \mathbf{V}^t;$ 
11      Update  $\mathbf{m}_n^{l,t}, \mathbf{v}_n^{l,t},$  and  $\mathbf{w}_n^{l,t}$  according to (4),
12        (5), and (3) over  $L$  epochs;
13      Compute  $\Delta\mathbf{M}_n^t \leftarrow \mathbf{m}_n^{L,t} - \mathbf{M}^t,$ 
14         $\Delta\mathbf{V}_n^t \leftarrow \mathbf{v}_n^{L,t} - \mathbf{V}^t, \Delta\mathbf{W}_n^t \leftarrow \mathbf{w}_n^{L,t} - \mathbf{W}^t;$ 
15      Sparsify  $\Delta\mathbf{M}_n^t, \Delta\mathbf{V}_n^t, \Delta\mathbf{W}_n^t$  as
16         $\Delta\hat{\mathbf{M}}_n^t \leftarrow \Delta\mathbf{M}_n^t \odot \mathbb{1}_{\text{SSM}_n^t},$ 
17         $\Delta\hat{\mathbf{V}}_n^t \leftarrow \Delta\mathbf{V}_n^t \odot \mathbb{1}_{\text{SSM}_n^t},$ 
18         $\Delta\hat{\mathbf{W}}_n^t \leftarrow \Delta\mathbf{W}_n^t \odot \mathbb{1}_{\text{SSM}_n^t},$  and upload the
19        SSM  $\mathbb{1}_{\text{SSM}_n^t}$  and the values of the
20        non-zero elements of  $\Delta\hat{\mathbf{M}}_n^t, \Delta\hat{\mathbf{V}}_n^t,$  and
21         $\Delta\hat{\mathbf{W}}_n^t$  to the server;
22  The server reconstructs  $\Delta\hat{\mathbf{M}}^t, \Delta\hat{\mathbf{V}}^t,$  and  $\Delta\hat{\mathbf{W}}^t$  with
23    the received values and  $\mathbb{1}_{\text{SSM}_n^t},$  and updates  $\Delta\hat{\mathbf{M}}^t,$ 
24     $\Delta\hat{\mathbf{V}}^t,$  and  $\Delta\hat{\mathbf{W}}^t$  according to FedAvg;

```

$O(3dq)$ in the standard FedAdam to $O(3kq+3d)$ in FedAdam-Top.

To further reduce the communication overhead, we propose to improve the FedAdam-Top algorithm by sparsifying the updates of local moment estimates and model parameters with an SSM. Denote the SSM by $\mathbb{1}_{\text{SSM}_n^t}$. Notably, $\mathbb{1}_{\text{SSM}_n^t} \in \{0, 1\}^d$ is a binary vector with exactly k ones and $d - k$ zeros. As shown in Algorithm 2, the proposed FedAdam-SSM algorithm sparsifies the updates $\Delta\mathbf{M}_n^t, \Delta\mathbf{V}_n^t,$ and $\Delta\mathbf{W}_n^t$ as follows:

$$\Delta\hat{\mathbf{M}}_n^t = \Delta\mathbf{M}_n^t \odot \mathbb{1}_{\text{SSM}_n^t}, \quad (10)$$

$$\Delta\hat{\mathbf{V}}_n^t = \Delta\mathbf{V}_n^t \odot \mathbb{1}_{\text{SSM}_n^t}, \quad (11)$$

$$\Delta\hat{\mathbf{W}}_n^t = \Delta\mathbf{W}_n^t \odot \mathbb{1}_{\text{SSM}_n^t}. \quad (12)$$

As such, each device in FedAdam-SSM transmits a total of 4 vectors to the centralized server, which includes an SSM $\mathbb{1}_{\text{SSM}_n^t}$, and 3 k -dimensional vectors containing the values of the non-zero elements of the sparse updates of local moment estimates and model parameters. The total number of bits for uplink data transmission per communication round in FedAdam-SSM is $N(3kq + d)$. Therefore, the uplink data transmission volume per communication round can be further reduced from $O(3kq + 3d)$ in FedAdam-Top to $O(3kq + d)$ in FedAdam-SSM.

V. DESIGN OF A SHARED SPARSE MASK

In this section, we optimize the SSM to mitigate the learning performance degradation caused by the sparsification error. We firstly derive an upper bound on the divergence between the local model trained by FedAdam-SSM and the desired model trained by centralized Adam. The divergence bound is related to the sparsification errors of the local model updates and moment estimates and the imbalanced data distribution. To mitigate the learning performance degradation caused by sparsification error, the main idea of designing the SSM is to minimize the divergence bound between FedAdam-SSM and centralized Adam.

A. Learning Performance Bound with Sparsification Error and Data Imbalance

Before the theoretical analysis, we make the following assumptions on the objective loss function.

Assumption 1: (Lipschitz continuous gradient). The loss function $f(\mathbf{w}, \mathcal{D}_n)$ is differentiable and $\nabla f(\mathbf{w}, \mathcal{D}_n)$ is ρ -Lipschitz continuous, i.e., for any $n \in \mathcal{N}$, and $\mathbf{x}, \mathbf{y} \in \mathbb{R}^d$, $\|\nabla f(\mathbf{x}, \mathcal{D}_n) - \nabla f(\mathbf{y}, \mathcal{D}_n)\| \leq \rho \|\mathbf{x} - \mathbf{y}\|$.

Assumption 2: (Bounded gradient). The loss function $f(\mathbf{w}, \xi)$ has G -bounded gradient, i.e., for any $\mathbf{w} \in \mathbb{R}^d$, $\xi \in \cup \mathcal{D}_n$, and $j \in [d]$, we have $|\nabla f(\mathbf{w}, \xi)_j| \leq G$.

Assumption 3: (Bounded local and global variances). For any $n \in \mathcal{N}$, $\xi \in \mathcal{D}_n$, and $\mathbf{w} \in \mathbb{R}^d$, the stochastic gradient $\nabla f(\mathbf{w}, \xi)$ has bounded variance, i.e., $\mathbb{E}[\|\nabla f(\mathbf{w}, \xi) - \nabla f(\mathbf{w}, \mathcal{D}_n)\|^2] \leq \sigma_l^2$. We also assume that the variance of gradient $\nabla f(\mathbf{w}, \mathcal{D}_n)$ is bounded, i.e., $\|\nabla f(\mathbf{w}, \mathcal{D}_n) - \nabla f(\mathbf{w}, \cup \mathcal{D}_n)\|^2 \leq \sigma_g^2$.

Note that **Assumption 1** on bounded smoothness and **Assumption 2** on bounded gradient are widely used in the FL community for convergence analysis [19], [27]–[29], [33]. In **Assumption 3**, the bounded variances of local and global gradients quantify the sampling noise and data distribution diversity among distributed devices in FL, respectively.

To facilitate our analysis, we first introduce several auxiliary notations. Let $\mathbf{M}^t, \mathbf{V}^t,$ and \mathbf{W}^t denote the non-sparse global moment estimates and model parameters at the beginning of the t -th communication round, i.e., $\mathbf{M}^t = \mathbf{M}^{t-1} + \frac{\sum_{n=1}^N |\mathcal{D}_n| \Delta\mathbf{M}_n^{t-1}}{\sum_{n=1}^N |\mathcal{D}_n|}, \mathbf{V}^t = \mathbf{V}^{t-1} + \frac{\sum_{n=1}^N |\mathcal{D}_n| \Delta\mathbf{V}_n^{t-1}}{\sum_{n=1}^N |\mathcal{D}_n|},$ and $\mathbf{W}^t = \mathbf{W}^{t-1} + \frac{\sum_{n=1}^N |\mathcal{D}_n| \Delta\mathbf{W}_n^{t-1}}{\sum_{n=1}^N |\mathcal{D}_n|}$. Let $\check{\mathbf{m}}^{l,t}, \check{\mathbf{v}}^{l,t},$ and $\check{\mathbf{w}}^{l,t}$ denote the auxiliary moment estimates and model parameters that follow the update rule of centralized Adam. To be specific, $\check{\mathbf{m}}^{l,t}, \check{\mathbf{v}}^{l,t},$ and $\check{\mathbf{w}}^{l,t}$ start from the non-sparse global moment estimates and model parameters $\mathbf{M}^t, \mathbf{V}^t,$ and \mathbf{W}^t , and update with the full global gradient descent $\nabla f(\check{\mathbf{w}}^{l,t}, \cup \mathcal{D}_n)$ as follows:

$$\check{\mathbf{m}}^{l+1,t} = \beta_1 \check{\mathbf{m}}^{l,t} + (1 - \beta_1) \nabla f(\check{\mathbf{w}}^{l,t}, \cup \mathcal{D}_n), \quad (13)$$

$$\check{\mathbf{v}}^{l+1,t} = \beta_2 \check{\mathbf{v}}^{l,t} + (1 - \beta_2) \left(\nabla f(\check{\mathbf{w}}^{l,t}, \cup \mathcal{D}_n) \right)^2, \quad (14)$$

$$\check{\mathbf{w}}^{l+1,t} = \check{\mathbf{w}}^{l,t} - \eta \frac{\check{\mathbf{m}}^{l+1,t}}{\sqrt{\check{\mathbf{v}}^{l+1,t} + \epsilon}}. \quad (15)$$

For ease of exposition, we define $D_n = |\mathcal{D}_n|, \tilde{D}_n = |\tilde{\mathcal{D}}_n|, \tilde{F}_n(\mathbf{w}) = f(\mathbf{w}, \tilde{D}_n), F_n(\mathbf{w}) = f(\mathbf{w}, D_n),$ and $F(\mathbf{w}) = f(\mathbf{w}, \cup \mathcal{D}_n)$.

Theorem 1: Suppose **Assumptions** 1, 2, and 3 hold. For any $n \in \mathcal{N}$, $l \in \mathcal{L}$, and $t \in \mathcal{T}$, the divergence between the local model trained by FedAdam-SSM and the desired model trained by centralized Adam can be bounded as follows:

$$\begin{aligned} & \|\mathbf{w}_n^{l,t} - \check{\mathbf{w}}^{l,t}\| \\ & \leq \Gamma \|\mathbf{W}^t - \check{\mathbf{W}}^t\| + \Lambda \|\mathbf{M}^t - \check{\mathbf{M}}^t\| + \Theta \|\mathbf{V}^t - \check{\mathbf{V}}^t\| + \Phi \\ & \leq \sum_{n=1}^N \frac{\bar{D}_n}{\sum_{n=1}^N \bar{D}_n} \left(\Gamma \left\| \left(1 - \mathbb{1}_{\text{SSM}_n^{t-1}}\right) \odot \Delta \mathbf{W}_n^{t-1} \right\| + \Lambda \left\| \left(1 - \mathbb{1}_{\text{SSM}_n^{t-1}}\right) \odot \Delta \mathbf{M}_n^{t-1} \right\| + \Theta \left\| \left(1 - \mathbb{1}_{\text{SSM}_n^{t-1}}\right) \odot \Delta \mathbf{V}_n^{t-1} \right\| \right) + \Phi, \end{aligned} \quad (16)$$

where

$$\begin{aligned} \Gamma &= \frac{1}{\sqrt{\psi^2 + 4\phi}} \left(\left(\frac{\psi - \sqrt{\psi^2 + 4\phi}}{2} \right)^l \left(\phi + \frac{\sqrt{\psi^2 + 4\phi} - \psi}{2} - \beta_1 (1 - \beta_2) \frac{dG^2 \eta \rho}{\epsilon \sqrt{\epsilon}} \right) + \left(\frac{\sqrt{\psi^2 + 4\phi} + \psi}{2} - \phi + \frac{dG^2 \eta \rho}{\epsilon \sqrt{\epsilon}} \beta_1 (1 - \beta_2) \right) \right. \\ & \quad \left. \times \left(\frac{\psi + \sqrt{\psi^2 + 4\phi}}{2} \right)^l \right), \end{aligned} \quad (17)$$

$$\Lambda = \frac{\eta \beta_1}{\sqrt{\epsilon} \sqrt{\psi^2 + 4\phi}} \left(\left(\frac{\psi + \sqrt{\psi^2 + 4\phi}}{2} \right)^l - \left(\frac{\psi - \sqrt{\psi^2 + 4\phi}}{2} \right)^l \right), \quad (18)$$

$$\Theta = \frac{\sqrt{d} G \eta \beta_2}{2 \epsilon \sqrt{\epsilon} \sqrt{\psi^2 + 4\phi}} \left(\left(\frac{\psi + \sqrt{\psi^2 + 4\phi}}{2} \right)^l - \left(\frac{\psi - \sqrt{\psi^2 + 4\phi}}{2} \right)^l \right), \quad (19)$$

and

$$\begin{aligned} \Phi &= \frac{\frac{\sigma_l}{\sqrt{D_n}} + \sigma_g}{\sqrt{\psi^2 + 4\phi}} \left(\frac{\eta}{\sqrt{\epsilon}} (1 - \beta_1) + \frac{dG^2 \eta}{\epsilon \sqrt{\epsilon}} (1 - \beta_2) \right) \left(\left(\frac{\psi + \sqrt{\psi^2 + 4\phi}}{2} \right)^l - \left(\frac{\psi - \sqrt{\psi^2 + 4\phi}}{2} \right)^l \right) \\ & \quad + \frac{\chi}{1 - \psi - \phi} \left(\frac{1}{\sqrt{\psi^2 + 4\phi}} \left(\left(1 - \frac{\psi + \sqrt{\psi^2 + 4\phi}}{2} \right)^l - \left(\frac{\psi - \sqrt{\psi^2 + 4\phi}}{2} \right)^l \right) + 1 \right). \end{aligned} \quad (20)$$

Note that ϕ , ψ and χ are given as

$$\phi = \frac{\beta_1}{\sqrt{\beta_2}}, \quad (21)$$

$$\psi = 1 + \frac{\beta_1}{\sqrt{\beta_2}} + \frac{\eta \rho (1 - \beta_1)}{\sqrt{\epsilon}} \left(1 + \frac{(1 - \beta_2) dG^2}{\epsilon} \right), \quad (22)$$

and

$$\begin{aligned} \chi &= dG\eta \left(\frac{2\beta_1 (1 - \sqrt{\beta_2})}{\epsilon \sqrt{\epsilon} \beta_2} (G^2 + \epsilon) + \frac{(1 - \beta_1) \beta_2}{\epsilon \sqrt{\epsilon}} G^2 \right) \\ & \quad + \frac{(1 - \beta_1) \eta \left(\frac{\sigma_l}{\sqrt{D_n}} + \sigma_g \right)}{\sqrt{\epsilon}} \left(1 + \frac{(1 - \beta_2) dG^2}{\epsilon} \right). \end{aligned} \quad (23)$$

Proof: See the proof in Section I in the supplementary material. ■

Remark 1: From **Theorem 1**, we can observe that the upper bound on $\|\mathbf{w}_n^{l,t} - \check{\mathbf{w}}^{l,t}\|$ is dominated by the term Φ and the weighted sum of $\|\mathbf{W}^t - \check{\mathbf{W}}^t\|$, $\|\mathbf{M}^t - \check{\mathbf{M}}^t\|$ and $\|\mathbf{V}^t - \check{\mathbf{V}}^t\|$ as follows:

- 1) The term Φ is determined by the variances of local and global gradient (i.e., $\frac{\sigma_l}{\sqrt{D_n}}$ and σ_g). Decreases in local and global gradient variances can contribute to a smaller divergence between the model parameters trained by FedAdam-SSM and centralized Adam, which indicates an improved learning performance in FedAdam-SSM training. This is consistent with the fact that FL performs better on IID datasets than non-IID datasets.
- 2) The weighted sum term reveals the impact of the sparsification of the updates of local model parameters and moment estimates on the learning performance of FedAdam-SSM. Specifically, lower sparsification errors of model parameters and moment estimates, i.e., $\|\mathbf{W}^t - \check{\mathbf{W}}^t\|$, $\|\mathbf{M}^t - \check{\mathbf{M}}^t\|$, and $\|\mathbf{V}^t - \check{\mathbf{V}}^t\|$, can lead to a reduced gap between $\mathbf{w}_n^{l,t}$ and $\check{\mathbf{w}}^{l,t}$, and thereby improving the learning performance of FedAdam-SSM. Given zero sparsification errors (i.e., $\|\mathbf{W}^t - \check{\mathbf{W}}^t\| = 0$, $\|\mathbf{M}^t - \check{\mathbf{M}}^t\| = 0$, and $\|\mathbf{V}^t - \check{\mathbf{V}}^t\| = 0$), the divergence between FedAdam-SSM and centralized Adam is reduced to the divergence between standard FedAdam and centralized Adam, i.e.,

$$\|\mathbf{w}_n^{l,t} - \check{\mathbf{w}}^{l,t}\| \leq \Phi, \quad (24)$$

which is exclusively related to the data distribution among the distributed devices.

Remark 2: **Theorem 1** also shows that for the same sparsification ratio, FedAdam-Top can achieve the lowest weighted sum of the sparsification errors by separately sparsifying the local updates $\Delta \mathbf{W}_n^t$, $\Delta \mathbf{M}_n^t$, and $\Delta \mathbf{V}_n^t$ with the top- k sparsifier. This indicates that the divergence between FedAdam-Top and centralized Adam serves as a lower bound on the divergence between sparse FedAdam and centralized Adam.

B. Optimal Shared Sparse Mask

From **Theorem 1**, the main idea of minimizing the divergence between the model parameters trained by FedAdam-SSM and centralized Adam is to minimize the weighted sum of the sparsification errors, i.e.,

$$\begin{aligned} & \Gamma \left\| \Delta \mathbf{W}_n^t \odot \left(1 - \mathbb{1}_{\text{SSM}_n^t}\right) \right\| + \Lambda \left\| \Delta \mathbf{M}_n^t \odot \left(1 - \mathbb{1}_{\text{SSM}_n^t}\right) \right\| \\ & \quad + \Theta \left\| \Delta \mathbf{V}_n^t \odot \left(1 - \mathbb{1}_{\text{SSM}_n^t}\right) \right\|. \end{aligned} \quad (25)$$

To this end, we next proceed to find an optimal SSM by comparing the magnitude of Γ , Λ and Θ as follows.

Proposition 1: If the exponential decay rate β_2 satisfies

$$\beta_2 < 1 - \frac{1}{1 + 2G\rho\sqrt{d}}, \quad (26)$$

then

$$\Gamma > \Theta > \Lambda. \quad (27)$$

Proof: See the proof in Section II in the supplementary material. ■

Remark 3: Notably, $\rho > 0$ is the Lipschitz constant, $d > 0$ is the number of model parameters, $\beta_2 \in [0, 1)$ is the exponential decay rate of the second moment estimate, and $G > 0$ is the upper bound on the stochastic gradient $|\nabla f(\mathbf{w}, \xi)|_j$. Given that d is typically an extremely large value, $1 - \frac{1}{1+2G\rho\sqrt{d}}$ approaches 1. Therefore, the inequality in (26) can be easily implemented since $\beta_2 \in [0, 1)$ is often set to 0.999 in the Adam optimizer.

From the theoretical and experimental analysis of model parameters and moment estimates produced by Adam [30], [34], [35], $\Delta \mathbf{W}_n^t$ is of a much larger order of magnitude than $\Delta \mathbf{M}_n^t$ and $\Delta \mathbf{V}_n^t$. Together with **Proposition 1**, it can be inferred that the term $\Gamma \left\| \Delta \mathbf{W}_n^t \odot \left(1 - \mathbb{1}_{\text{SSM}_n^t} \right) \right\|$ is the major contributor to the divergence between FedAdam-SSM and centralized Adam. Therefore, the minimization of the weighted sum of the sparsification errors in (25) can be equivalently transformed into the minimization of $\left\| \Delta \mathbf{W}_n^t \odot \left(1 - \mathbb{1}_{\text{SSM}_n^t} \right) \right\|$. As such, an optimal SSM can be determined by sparsifying the update of local model parameters with the top- k sparsifier, i.e.,

$$\mathbb{1}_{\text{SSM}_n^t} = \mathbb{1}_{\text{Top}_k} \left(\Delta \mathbf{W}_n^t \right). \quad (28)$$

With this optimal SSM, the proposed FedAdam-SSM can effectively mitigate the learning performance degradation caused by the sparsification error.

VI. CONVERGENCE ANALYSIS

In this section, we analyze the convergence of the proposed FedAdam-SSM in both convex and non-convex settings.

We first present the convergence of FedAdam-SSM for general non-convex loss functions as follows.

Theorem 2: (Non-convexity). Suppose **Assumptions 1, 2, and 3** hold. Then, after running FedAdam-SSM for T communication rounds, we have

$$\begin{aligned} \frac{1}{T} \sum_{t=0}^{T-1} \|\nabla F(\mathbf{W}^t)\|^2 &\leq \frac{2}{\eta T} \left(F(\mathbf{W}^0) - F(\mathbf{W}^T) \right) + 2((\eta\rho+2)(1-\alpha) \\ &+ \eta\rho - 1) \frac{\eta G^2 d L^2}{\epsilon} + 6G^2 d \left(\left(L - \frac{\beta_2(1-(\beta_2)^L)}{1-\beta_2} \right) \frac{G^4 d L}{4\epsilon^3} + \frac{L^2}{\epsilon} \right. \\ &\left. + \frac{4\beta_1(1-(\beta_1)^L)}{\epsilon(1-\beta_1)^2} + 1 + \frac{\rho^2 L^2}{3\epsilon} \right) + 6 \sum_{n=1}^N \frac{\tilde{D}_n \left(\frac{\sigma_l}{\sqrt{\tilde{D}_n}} + \sigma_g \right)^2}{\sum_{n=1}^N \tilde{D}_n}. \quad (29) \end{aligned}$$

Proof: See the proof in Section III in the supplementary material. ■

Remark 4: The convergence rate upper bound of FedAdam-SSM given in **Theorem 2** includes a vanishing part as the sparsification ratio α increases and a constant part involving the local and global variances σ_l and σ_g caused by sampling noise and heterogeneous distributed datasets. This coincides with our intuitive understanding: 1) A lower sparsification ratio

can contribute to a reduced sparsification error, and thereby an improved model performance. 2) Non-IID data distributions can result in a global model that produces shifted gradients on local datasets, leading to degraded model accuracy.

Proposition 2: Assume **Assumptions 1, 2, and 3** hold, and let the learning rate $\eta = O\left(\frac{1}{L^2\sqrt{T}}\right)$. Then, for FedAdam-SSM, it holds that

$$\begin{aligned} \frac{1}{T} \sum_{t=0}^{T-1} \|\nabla F(\mathbf{W}^t)\|^2 &\leq O\left(\frac{(F(\mathbf{W}^0) - F(\mathbf{W}^T)) L^2}{\sqrt{T}}\right) \\ &+ O\left(\frac{(1-\alpha)G^2d}{\epsilon\sqrt{T}}\right) + O\left(\frac{(1-\alpha)\rho G^2d}{\epsilon L^2 T}\right). \quad (30) \end{aligned}$$

Remark 5: From **Proposition 2**, we can see that when the communication round T is sufficiently large, the dominant term of the asymptotic convergence rate of FedAdam-SSM achieves a linear speedup of $O\left(\frac{1}{\sqrt{T}}\right)$. This indicates that to reach any error $\delta > 0$, the FedAdam-SSM algorithm needs $O\left(\frac{1}{\delta^2}\right)$ communication rounds on non-convex loss functions.

Remark 6: From **Proposition 2**, it can be seen that when $L < \left(\frac{(1-\alpha)\rho G^2 d}{\epsilon(F(\mathbf{W}^0) - F(\mathbf{W}^T))\sqrt{T}}\right)^{\frac{1}{4}}$, the term $O\left(\frac{(1-\alpha)\rho G^2 d}{\epsilon L^2 T}\right)$ dominates the given bound on convergence of FedAdam-SSM, which indicates that the convergence rate of FedAdam-SSM can be improved by increasing local epoch L . This phenomenon is consistent with our intuitive understanding that using a large local epoch L can lead to a local minimizer and thereby speed up the training process of FedAdam-SSM. However, there is a point where increasing local epoch L too much can degrade the model accuracy and consequently slow down the convergence rate. When $L > \left(\frac{(1-\alpha)\rho G^2 d}{\epsilon(F(\mathbf{W}^0) - F(\mathbf{W}^T))\sqrt{T}}\right)^{\frac{1}{4}}$, the dominant term becomes $O\left(\frac{(F(\mathbf{W}^0) - F(\mathbf{W}^T))L^2}{\sqrt{T}}\right)$. In this case, a large local epoch L can lead to a strong device drift, which degrades the training performance of FedAdam-SSM. The above discussion provides guidance for selecting an appropriate value of L to speed up the convergence rate.

In the following, we present the convergence of FedAdam-SSM under the Polyak-Łojasiewicz (PŁ) condition.

Assumption 4: (PŁ condition). The objective loss function $F(\mathbf{w})$ satisfies a PŁ- μ inequality, i.e., $\|\nabla F(\mathbf{w})\|^2 \geq 2\mu(F(\mathbf{w}) - F(\mathbf{w}^*))$, $\forall \mathbf{w} \in \mathbb{R}^d$.

Theorem 3: (PŁ condition). Suppose **Assumptions 1, 2, 3, and 4** hold. Then, after running FedAdam-SSM for T communication rounds, we have

$$\begin{aligned} F(\mathbf{W}^T) - F(\mathbf{w}^*) &\leq (1 - \eta\mu)^T \left(F(\mathbf{W}^0) - F(\mathbf{w}^*) \right) + \frac{\eta G^2 d L^2}{\mu\epsilon} \\ &((\eta\rho+2)(1-\alpha) + \eta\rho - 1) + \frac{3G^2 d}{\mu} \left(\frac{4\beta_1(1-(\beta_1)^L)}{\epsilon(1-\beta_1)^2} + \frac{L^2}{\epsilon} + \frac{\rho^2 L^2}{3\epsilon} \right. \\ &\left. + 1 + \frac{G^4 d L}{4\epsilon^3} \left(L - \frac{\beta_2(1-(\beta_2)^L)}{1-\beta_2} \right) \right) + \frac{3}{\mu} \sum_{n=1}^N \frac{\tilde{D}_n \left(\frac{\sigma_l}{\sqrt{\tilde{D}_n}} + \sigma_g \right)^2}{\sum_{n=1}^N \tilde{D}_n}. \quad (31) \end{aligned}$$

Proof: See the proof in Section IV in the supplementary material. ■

Remark 7: From **Theorem 3**, it can be inferred that, under the PL condition, a small learning rate can slow down the convergence speed, while a large learning rate can compromise the model accuracy. Specifically, a small learning rate η can result in a slow decay of the term $(1 - \eta\mu)^T (F(\mathbf{W}^0) - F(\mathbf{w}^*))$, thereby yielding a deceleration of the training process. On the other hand, using a large learning rate η can contribute to an increased term $\frac{((\eta\rho+2)(1-\alpha)+\eta\rho-1)\eta G^2 d L^2}{\mu\epsilon}$, thereby leading to degraded model accuracy. This is consistent with our intuitive understanding that a small η can cause the optimizer to converge slowly, while a large η can cause drastic updates which can lead to divergent behaviour.

Proposition 3: Suppose **Assumptions 1, 2, 3, and 4** hold, and let the learning rate $\eta = \mathcal{O}\left(\frac{\ln T}{L^2 T}\right)$. After running the FedAdam-SSM algorithm, it holds that that

$$F(\mathbf{W}^T) - F(\mathbf{w}^*) \leq \tilde{\mathcal{O}}\left(\frac{F(\mathbf{W}^0) - F(\mathbf{w}^*)}{T}\right) + \tilde{\mathcal{O}}\left(\frac{\rho G^2 d}{\mu\epsilon L^2 T^2}\right) + \tilde{\mathcal{O}}\left((1 - \alpha)\frac{G^2 d}{\mu\epsilon T}\right). \quad (32)$$

Proof: See the proof in Section V in the supplemental material. ■

Remark 8: From **Proposition 3**, we can observe that under the PL condition, the convergence rate of the FedAdam-SSM algorithm can be improved to $\mathcal{O}\left(\frac{1}{T}\right)$ by setting $\eta = \mathcal{O}\left(\frac{\ln T}{L^2 T}\right)$. That is, under the PL condition, FedAdam-SSM only requires $\mathcal{O}\left(\frac{1}{\delta}\right)$ communication rounds to reach an error $\delta > 0$.

VII. EXPERIMENTAL RESULTS

A. Experimental Settings

To evaluate the FL performance of the proposed FedAdam-SSM algorithm, we train a CNN on the Fashion-MNIST dataset, VGG-11 on the CIFAR-10 dataset, and ResNet-18 on the SVHN dataset with IID and non-IID settings to demonstrate the training efficiency.

Datasets and models. 1) Fashion-MNIST consists of a training set of 60000 28×28 grayscale images belonging to 10 different classes, and a test set of 10000 images. 2) CIFAR-10 consists of 60000 32×32 RGB images in 10 classes (from 0 to 9), with 5000 training images and 1000 test images per class. 3) SVHN contains over 60000 32×32 RGB images in 10 classes (from 0 to 9), which is cropped from real-world pictures of house number plates. For the Fashion-MNIST dataset, we adopt a CNN model with two 5×5 convolutional layers (each followed by ReLU activation and a 2×2 max pooling layer), two fully connected layers, and a final softmax output layer. For the CIFAR-10 dataset, we adopt a VGG-11 model that consists of eight 3×3 convolutional layers, three fully connected layers, and a final softmax output layer. For the SVHN dataset, we adopt a ResNet-18 model that consists of a 2×2 convolutional layer, two pooling layers, eight residual units (each with two 3×3 convolutional layers), a fully connected layer, and a final softmax output layer.

Data distribution. For non-IID settings, we follow the previous works [36], [37] to split the local datasets using the Dirichlet distribution with a concentration parameter $\theta = 0.1$.

Note that the lower the concentration parameter, the higher the non-IID degree of the data distribution.

Implementation. In our experiments, we set the number of distributed devices $N = 20$, local epoch $L = 30$, learning rate $\eta = 0.001$, and sparsification ratio $\alpha = 0.05$. For the Adam optimizer, we set $\beta_1 = 0.9$, $\beta_2 = 0.999$, and $\epsilon = 10^{-6}$. As previously stated, FedAdam-SSM uploads the SSM to the centralized server to represent the position of each non-zero element in the sparse vectors. Alternatively, we could upload the indices of these non-zero elements to represent their positions instead of uploading the SSM. This method necessitates $\log_2(d)$ bits to inform the centralized server of the index of each non-zero element within the d -dimensional sparse vector [38], [39]. In our experiment, we employ both methods and select the one with the lower communication overhead. Therefore, the total number of bits for uplink data transmission per communication round in FedAdam-SSM and FedAdam-Top is $\min\{N(3kq + d), Nk(3q + \log_2(d))\}$ and $\min\{3N(kq + d), 3Nk(q + \log_2(d))\}$, respectively.

Baselines. For comparison purpose, we consider the following baseline algorithms: 1) FedAdam (See Algorithm 1), 2) FedAdam-Top, 3) 1-bit Adam [29], 4) Efficient Adam [28], 5) Fairness-top [40], 6) FedAdam-SSM_M, and 6) FedAdam-SSM_V. FedAdam is in fact a special case of FedAdam-SSM and FedAdam-Top when we set the sparsification ratio α to 1. 1-bit Adam follows a two-stage training paradigm: a) first run vanilla Adam as a warm-up, where the local moment estimates and model parameters are communicated with full precision; b) then fix the second moment estimate as a precondition and communicate the first moment estimates with error-compensated 1-bit quantization. Efficient Adam utilizes a two-way quantization scheme to reduce the communication overhead and a two-way error feedback strategy to compensate for quantization errors. Fairness-top, FedAdam-SSM_M and FedAdam-SSM_V employ an SSM to sparsify the local moment estimates and model parameters, thereby reducing the uplink communication overhead. In Fairness-top, the SSM is determined by sparsifying the union of the local moment estimates and model parameters with the top- k sparsifier. FedAdam-SSM_M and FedAdam-SSM_V determine the SSM by sparsifying the local first moment estimates and the second moment estimates with the top- k sparsifier, respectively.

B. Results and Discussion

1) *Comparison of Values of $\Delta \mathbf{W}_n^t$, $\Delta \mathbf{M}_n^t$ and $\Delta \mathbf{V}_n^t$:* To demonstrate the magnitude of the update of model parameters and moment estimates (i.e., $\Delta \mathbf{W}_n^t$, $\Delta \mathbf{M}_n^t$, and $\Delta \mathbf{V}_n^t$), Fig. 1 compares the probability density of their logarithmic values on different datasets and models. From Fig. 1, we can observe that the logarithms of $\Delta \mathbf{W}_n^t$, $\Delta \mathbf{M}_n^t$ and $\Delta \mathbf{V}_n^t$ appear to approximately follow normal distributions with different means and variances, and the logarithmic values indicate that $\Delta \mathbf{W}_n^t > \Delta \mathbf{M}_n^t > \Delta \mathbf{V}_n^t$. Specifically, for CNN on Fashion-MNIST, Fig. 1 (a) shows that the logarithms of $\Delta \mathbf{W}_n^t$, $\Delta \mathbf{M}_n^t$ and $\Delta \mathbf{V}_n^t$ exhibit approximate normal distributions centered around -2 , -3 and -6 , respectively. For ResNet-18 on SVHN,

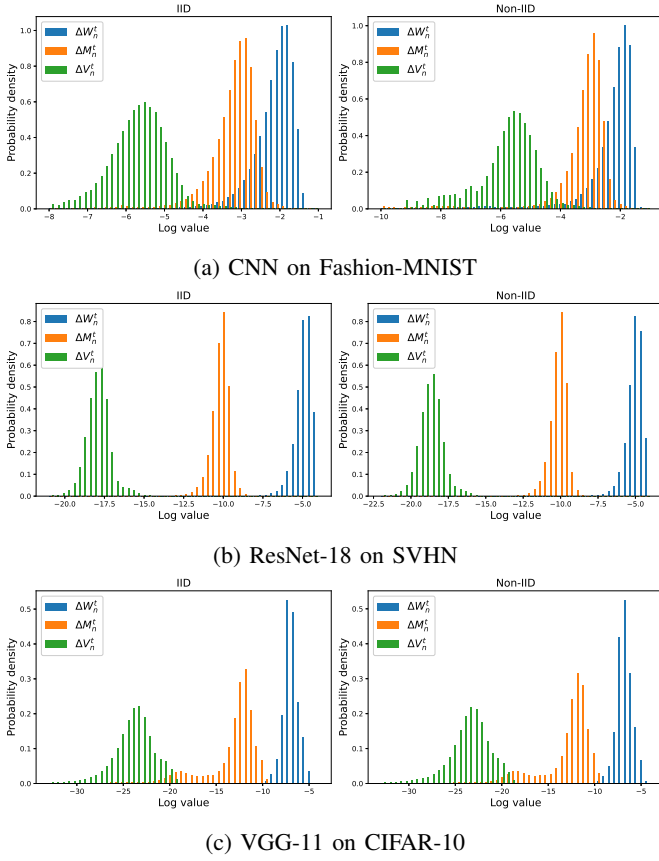


Fig. 1: Probability density of the log value of ΔW_n^t , ΔM_n^t and ΔV_n^t on different models and datasets.

Fig. 1 (b) indicates that the logarithms of ΔW_n^t , ΔM_n^t and ΔV_n^t fall within their respective ranges of -7.5 to -4 , -12.5 to -8 , and -20 to -15 , respectively. For VGG-11 on CIFAR-10, Fig. 1 (c) illustrates that the logarithms of ΔW_n^t , ΔM_n^t and ΔV_n^t lie in the ranges of -10 to -5 , -25 to -10 , and -35 to -20 , respectively. Therefore, the experimental results verify that the update of model parameters (i.e., ΔW_n^t) is significantly larger in magnitude compared to the updates of moment estimates (i.e., ΔM_n^t and ΔV_n^t), which is also consistent with the theoretical and experimental analysis of model parameters and moment estimates produced by Adam [30], [34], [35].

2) Performance Comparison with Baseline Algorithms:

Fig. 2 compares the model accuracy versus communication overhead between FedAdam-SSM and baseline algorithms. For CNN on Fashion-MNIST, the improvement in test accuracy compared to FedAdam-Top, Fairness-Top, FedAdam-SSM_M, FedAdam-SSM_V, FedAdam, 1-bit Adam and Efficient Adam is approximately 1.3%, 2.9%, 8.2%, 10.9%, 3.7%, 14.4%, 21.8% in the IID setting, and 1.8%, 2.5%, 9.7%, 10.7%, 11.7%, 17.3%, 39.3% in the Non-IID setting. For ResNet on SVHN, the improvement in test accuracy compared to FedAdam-Top, Fairness-Top, FedAdam-SSM_M, FedAdam-SSM_V, FedAdam, 1-bit Adam and Efficient Adam is approximately 4.5%, 1.1%, 9.6%, 1.9%, 2.3%, 22%, 23.1% in the IID setting, and 4.3%, 2.9%, 10.7%, 5.1%, 6.4%, 20.2%,

24.9% in the Non-IID setting. For VGG-11 on CIFAR-10, the improvement in test accuracy compared to FedAdam-Top, Fairness-Top, FedAdam-SSM_M, FedAdam-SSM_V, FedAdam, 1-bit Adam and Efficient Adam is approximately 4.1%, 1.5%, 3.8%, 10.7%, 4.8%, 15.2%, 14.4% in the IID setting, and 2.7%, 5.9%, 6.1%, 18.4%, 5.9%, 36.5%, 39.6% in the Non-IID setting. Table I compares the convergence rate of FedAdam-SSM and baseline algorithms.

From Fig. 2 and Table I, we can observe that in the context of both IID and Non-IID data distribution settings, FedAdam-SSM outperforms baseline algorithms both on model accuracy and convergence rate. The observations are listed as follows. First, FedAdam-SSM outperforms its counterparts among the sparse FedAdam algorithms both on test accuracy and convergence rate, including FedAdam-SSM_M, FedAdam-SSM_V, and Fairness-top. The improvement in test accuracy is approximately 3.8% ~ 10.9% compared to FedAdam-SSM_M, 1.9% ~ 18.4% compared to FedAdam-SSM_V, and 1.3% ~ 4.5% compared to FedAdam-Top on different models and datasets. Additionally, FedAdam-SSM achieves approximately over 2.19× convergence rate improvements over FedAdam-SSM_M, over 2.77× convergence rate improvements over FedAdam-SSM_V, and over 1.1× convergence rate improvements over FedAdam-SSM_M. Notably, FedAdam-SSM, FedAdam-SSM_M, FedAdam-SSM_V, and Fairness-top employ different SSMs to introduce sparsity in the updates of local model parameters and moment estimates, and maintain an identical communication overhead of $O(3kq + d)$. This observation highlights that the proposed SSM outperforms the alternative SSMs in terms of model accuracy and convergence rate. This is because our proposed SSM minimizes the divergence between centralized Adam and sparse FedAdam, which is consistent with Theorem 1. With the same sparsification ratio as FedAdam-SSM_M, FedAdam-SSM_V, and Fairness-top, the proposed SSM effectively reduces the sparsification error, thereby improving both model accuracy and convergence rate.

Second, it can be observed that FedAdam-SSM prevails slightly over FedAdam-Top and Fairness-Top in terms of test accuracy and convergence rate. Furthermore, FedAdam-SSM requires a significantly lower computational complexity compared to FedAdam-Top and Fairness-Top. To be specific, FedAdam-SSM improves test accuracy approximately 1.3% ~ 4.5% compared to FedAdam-Top and 1.1% ~ 2.9% compared to Fairness-Top on different models and datasets. The improvement in convergence rate is approximately 1.37× ~ 5.59× over FedAdam-Top, and 1.10× ~ 2.74× over Fairness-Top. Note that FedAdam-SSM determines the SSM by applying top- k sparsification to local model parameters. In contrast, Fairness-top determines the SSM by sparsifying the union of local model parameters and moment estimates with the top- k sparsifier. FedAdam-Top separately sparsifies the local model parameters and moment estimates using the top- k sparsification method. Therefore, the computational complexity of FedAdam-SSM, FedAdam-Top, and Fairness-Top can be represented as $O(d \log(k))$, $O(3d \log(k))$, and $O(9dk)$, respectively. FedAdam-SSM reduces the computational complexity by over 66.6% compared to both FedAdam-Top and Fairness-Top.

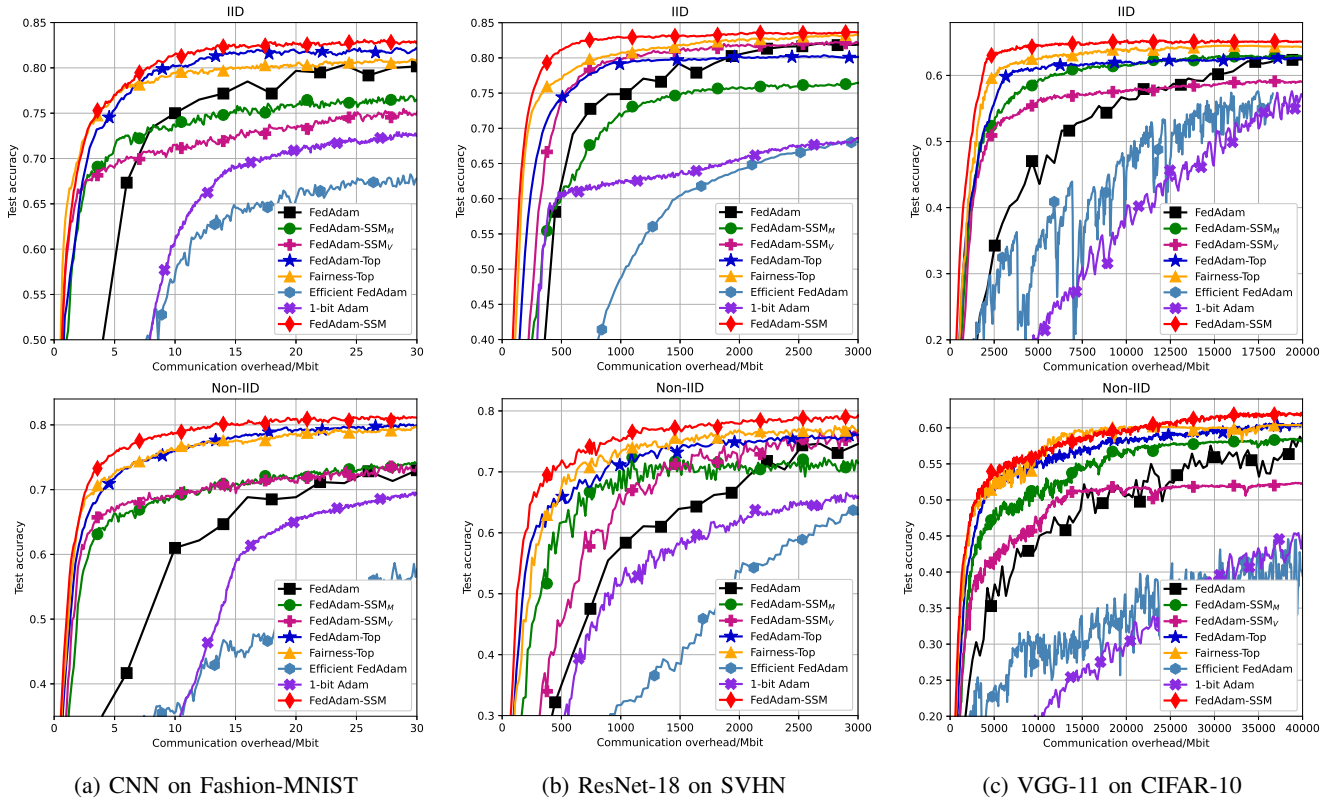


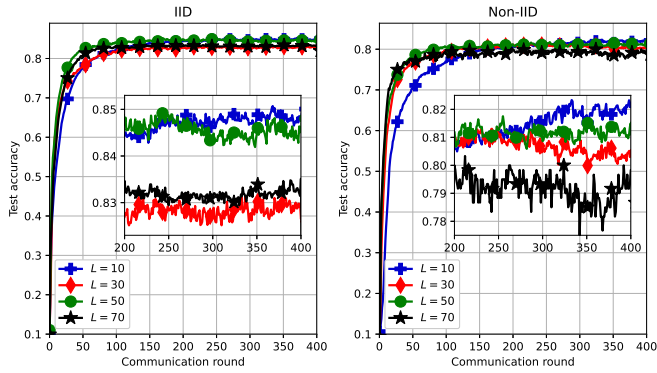
Fig. 2: The comparison of model accuracy versus communication overhead between FedAdam-SSM and baseline algorithms on different models and datasets.

TABLE I: Convergence rate of FedAdam-SSM and baseline algorithms on different models and datasets. “Acc.” represents the target test accuracy. “Comm.” represents the minimum communication overhead required to achieve the target test accuracy. ∞ means it is impossible to achieve the target test accuracy during the training process.

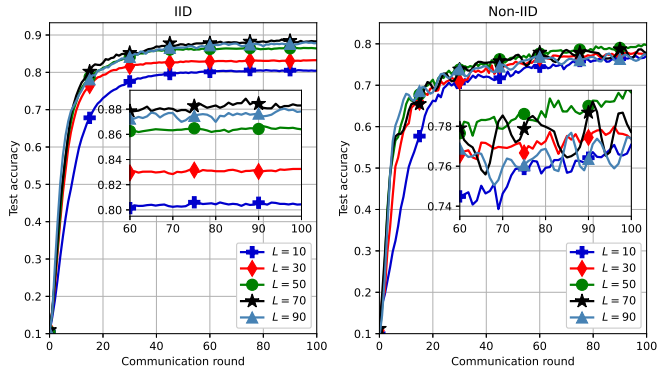
Setting	Algorithm	CNN on Fashion-MNIST		ResNet on SVHN		VGG-11 on CIFAR-10	
		Acc. (%)	Comm. (Mbit)	Acc. (%)	Comm. (Mbit)	Acc. (%)	Comm. (Mbit)
IID	FedAdam-SSM		8.15		591.0		2073.0
	FedAdam-Top		11.3 (1.39 \times)		1959.1 (3.31 \times)		11605.0 (5.59 \times)
	Fairness-Top		17.1 (2.09 \times)		1623.0 (2.74 \times)		4327.0 (2.09 \times)
	FedAdam-SSM _M	80.4	∞	80.2	∞	62.4	11651.0 (5.62 \times)
	FedAdam-SSM _V		∞		1870.7 (3.16 \times)		∞
	FedAdam		24.0 (2.94 \times)		2641.8 (4.47 \times)		18559.0 (8.95 \times)
	1-bit Adam		∞		∞		∞
	Efficient Adam		∞		∞		∞
Non-IID	FedAdam-SSM		13.0		737.3		8161.0
	FedAdam-Top		24.5 (1.88 \times)		1521.1 (2.06 \times)		11172.0 (1.37 \times)
	Fairness-Top		31.5 (2.42 \times)		1059.3 (1.44 \times)		8966.0 (1.10 \times)
	FedAdam-SSM _M	79.8	∞	74.4	∞	56.2	17951.0 (2.19 \times)
	FedAdam-SSM _V		∞		2042.1 (2.77 \times)		∞
	FedAdam		70.0 (5.38 \times)		2556.0 (3.47 \times)		27400.0 (3.36 \times)
	1-bit Adam		∞		∞		∞
	Efficient Adam		∞		∞		∞

Third, we can observe that FedAdam-SSM significantly outperforms the quantized FedAdam algorithms, i.e., 1-bit Adam and Efficient Adam, in terms of test accuracy and convergence rate. Specifically, the improvement in test accuracy is approximately 15.2% ~ 36.5% compared to 1-bit

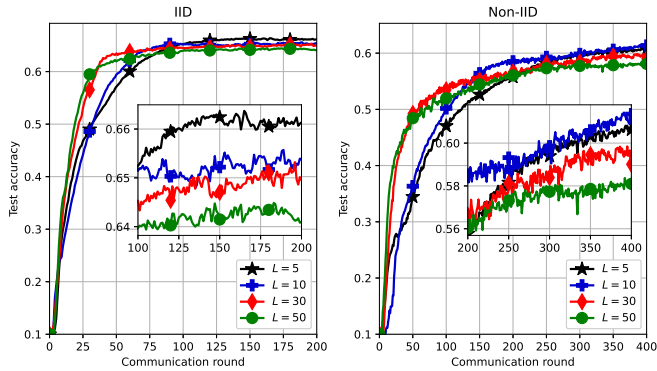
Adam, and 14.5% ~ 39.6% compared to Efficient Adam on different models and datasets. In addition, we can see that compared to the Non-IID setting, FedAdam-SSM achieves higher test accuracy and faster convergence rate in the IID data distribution setting. This is due to the fact that non-IID



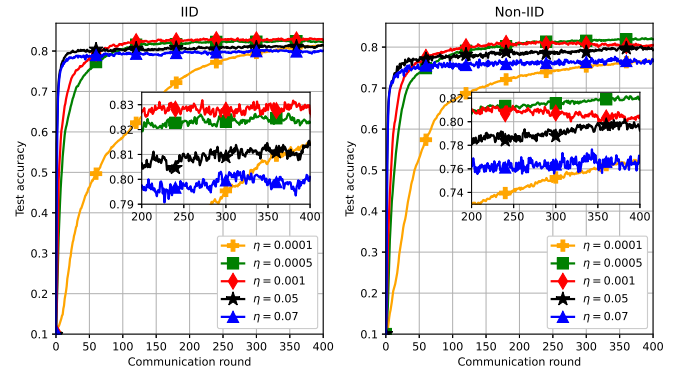
(a) CNN on Fashion-MNIST



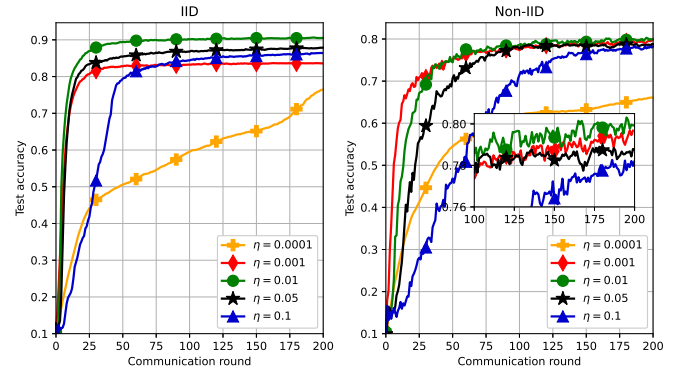
(b) ResNet-18 on SVHN



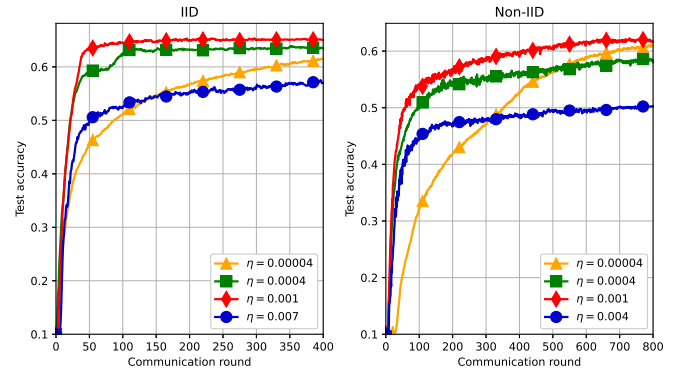
(c) VGG-11 on CIFAR-10



(a) CNN on Fashion-MNIST



(b) ResNet-18 on SVHN



(c) VGG-11 on CIFAR-10

Fig. 3: Model accuracy of FedAdam-SSM for different local epoch L on different models and datasets.

Fig. 4: Model accuracy of FedAdam-SSM for different learning rate η on different models and datasets.

data distributions can result in a global model that produces shifted gradients on local datasets, and thereby a degraded model accuracy. This observation is consistent with Theorem 2 that lower local and global variances σ_l and σ_g can lead to improved training performance.

3) *Sensitivity to Hyperparameters*: **Local epoch** measures the progress of local gradient descent. Fig. 3 plots the test accuracy of FedAdam-SSM for different values of local epoch L . From Fig. 3, we can see that the convergence rate shows a decreasing trend as L increases. Additionally, the test accuracy shows an initial increasing trend followed by a subsequent decrease as L increases. This is due to the fact that increasing local epoch L can lead to a local minimizer and thereby

improve the convergence rate. On the other hand, increasing L too much can lead to a strong device drift, which compromises the model accuracy and slows down the convergence. This observation highlights a trade-off in selecting the appropriate value of L to balance the convergence rate and model accuracy, which is consistent with Proposition 2.

Learning rate determines the step size in each gradient descent iteration while moving towards the minimum of the loss function. Fig. 4 plots the test accuracy of FedAdam-SSM for different learning rate η on different models and datasets. We can observe that on the one hand, increasing the learning rate η can improve the test accuracy and speed up the convergence. On the other hand, a too large η compromises the

model accuracy and consequently degrades the convergence rate. This is due to the fact that a small η can cause the optimizer to converge slowly or get stuck in plateaus or undesirable local minima, while a large η can cause drastic updates which can lead to divergent behaviour. The above discussion highlights a guidance for selecting an appropriate value of η to optimize the training performance, which is consistent with Theorem 3.

Sparsification ratio measures the sparsification error in the training process. Fig. 5 plots the test accuracy of FedAdam-SSM for different sparsification ratio α on different models and datasets. It can be observed that increasing the learning rate η can improve the test accuracy and speed up the convergence. This aligns with the findings of Theorem 2, demonstrating that a decreased sparsification ratio is associated with a diminished sparsification error, consequently leading to enhanced training performance.

VIII. CONCLUSION

In this paper, we have proposed a novel sparse FedAdam algorithm called FedAdam-SSM, which incorporates an SSM into the sparsification of the updates of local model parameters and moment estimates to reduce the uplink communication overhead. We have provided an upper bound on the divergence between the local model trained by FedAdam-SSM and the desired model trained by centralized Adam, which is related to the sparsification error and imbalanced data distribution. Based on this divergence bound, we have optimized the SSM to mitigate the learning performance degradation caused by the sparsification error. We have provided convergence bounds for the proposed FedAdam-SSM with both non-convex and convex objective function settings. We have investigated the impact of local epoch, learning rate and sparsification ratio on the convergence rate of FedAdam-SSM, and provided guidances for selecting appropriate values of local epoch, learning rate and sparsification ratio to improve the training performance. Extensive experiments on Fashion-MNIST, SVHN and CIFAR-10 datasets have verified the theoretical analysis and showed that FedAdam-SSM outperforms baselines in terms of both convergence rate and test accuracy. This work represents the first attempt to design the SSM for the sparsification of local model updates and moment estimates in sparse FedAdam and to provide a corresponding theoretical analysis.

REFERENCES

- [1] B. A. Salau, A. Rawal, and D. B. Rawat, "Recent advances in artificial intelligence for wireless internet of things and cyber-physical systems: A comprehensive survey," *IEEE Internet Things J.*, vol. 9, no. 15, pp. 12 916–12 930, 2022.
- [2] Z. Chang, S. Liu, X. Xiong, Z. Cai, and G. Tu, "A survey of recent advances in edge-computing-powered artificial intelligence of things," *IEEE Internet Things J.*, vol. 8, no. 18, pp. 13 849–13 875, 2021.
- [3] S. B. Baker and W. Xiang, "Artificial intelligence of things for smarter healthcare: A survey of advancements, challenges, and opportunities," *IEEE Commun. Surv. Tutorials*, vol. 25, no. 2, pp. 1261–1293, 2023.
- [4] T. Zhang, L. Gao, C. He, M. Zhang, B. Krishnamachari, and A. S. Avestimehr, "Federated learning for the internet of things: Applications, challenges, and opportunities," *IEEE Internet Things Mag.*, vol. 5, no. 1, pp. 24–29, 2022.
- [5] S. B. Baker and W. Xiang, "Artificial intelligence of things for smarter healthcare: A survey of advancements, challenges, and opportunities," *IEEE Commun. Surv. Tutorials*, vol. 25, no. 2, pp. 1261–1293, 2023.

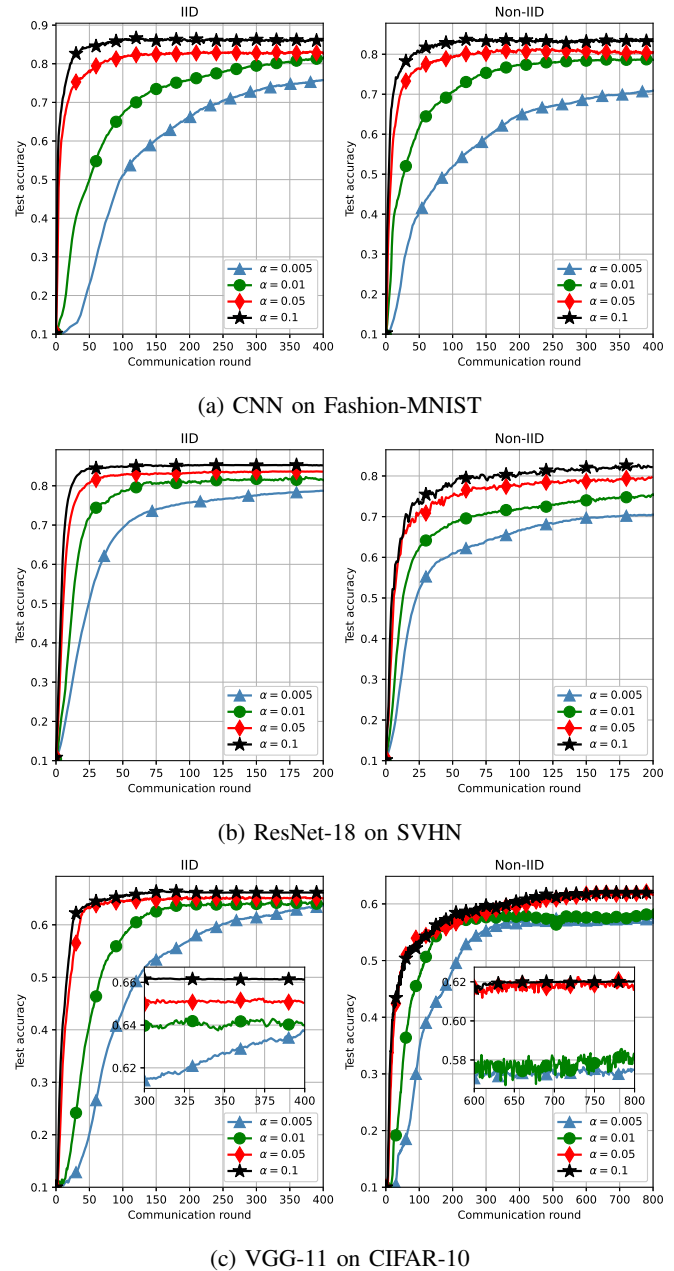


Fig. 5: Model accuracy of FedAdam-SSM for different sparsification ratio α on different models and datasets.

- [6] J. Li, Y. Shao, K. Wei, M. Ding, C. Ma, L. Shi, Z. Han, and H. V. Poor, "Blockchain assisted decentralized federated learning (BLADE-FL): performance analysis and resource allocation," *IEEE Trans. Parallel Distributed Syst.*, vol. 33, no. 10, pp. 2401–2415, 2022.
- [7] M. Ali, F. Naeem, M. Tariq, and G. Kaddoum, "Federated learning for privacy preservation in smart healthcare systems: A comprehensive survey," *IEEE J. Biomed. Health Informatics*, vol. 27, no. 2, pp. 778–789, 2023.
- [8] X. Deng, J. Li, C. Ma, K. Wei, L. Shi, M. Ding, and W. Chen, "Low-latency federated learning with DNN partition in distributed industrial iot networks," *IEEE J. Sel. Areas Commun.*, vol. 41, no. 3, pp. 755–775, 2023.
- [9] J. Bian, A. A. Arafat, H. Xiong, J. Li, L. Li, H. Chen, J. Wang, D. Dou, and Z. Guo, "Machine learning in real-time internet of things (iot) systems: A survey," *IEEE Internet Things J.*, vol. 9, no. 11, pp. 8364–8386, 2022.
- [10] M. Wang, W. Fu, X. He, S. Hao, and X. Wu, "A survey on large-scale

- machine learning,” *IEEE Trans. Knowl. Data Eng.*, vol. 34, no. 6, pp. 2574–2594, 2022.
- [11] X. He, F. Xue, X. Ren, and Y. You, “Large-scale deep learning optimizations: A comprehensive survey,” *CoRR*, vol. abs/2111.00856, 2021.
 - [12] B. Tran, S. Rossi, D. Milios, and M. Filippone, “All you need is a good functional prior for bayesian deep learning,” *J. Mach. Learn. Res.*, vol. 23, pp. 74:1–74:56, 2022.
 - [13] Z. Yang, W. Bao, D. Yuan, N. H. Tran, and A. Y. Zomaya, “Federated learning with nesterov accelerated gradient,” *IEEE Trans. Parallel Distributed Syst.*, vol. 33, no. 12, pp. 4863–4873, 2022.
 - [14] Y. Zhou, Q. Ye, and J. Lv, “Communication-efficient federated learning with compensated overlap-FedAvg,” *IEEE Trans. Parallel Distributed Syst.*, vol. 33, no. 1, pp. 192–205, 2022.
 - [15] C. T. Dinh, N. H. Tran, T. D. Nguyen, W. Bao, A. Y. Zomaya, and B. B. Zhou, “Federated learning with proximal stochastic variance reduced gradient algorithms,” in *Proceedings of the 49th International Conference on Parallel Processing*, Edmonton, AB, Canada, August 17–20, 2020, pp. 1–11.
 - [16] H. Zhu and Q. Ling, “Byzantine-robust aggregation with gradient difference compression and stochastic variance reduction for federated learning,” in *Proceedings of the IEEE International Conference on Acoustics, Speech and Signal Processing*, Virtual and Singapore, May 23–27, 2022, pp. 4278–4282.
 - [17] T. Chen, Z. Guo, Y. Sun, and W. Yin, “CADAA: communication-adaptive distributed Adam,” in *Proceedings of the 24th International Conference on Artificial Intelligence and Statistics*, Virtual Event, April 13–15, 2021, pp. 613–621.
 - [18] S. Li, Q. Qi, J. Wang, H. Sun, Y. Li, and F. R. Yu, “GGs: general gradient sparsification for federated learning in edge computing,” in *Proceedings of the IEEE International Conference on Communications*, Dublin, Ireland, June 7–11, 2020, pp. 1–7.
 - [19] W. Xian, F. Huang, and H. Huang, “Communication-efficient Adam-type algorithms for distributed data mining,” in *Proceedings of the IEEE International Conference on Data Mining*, Orlando, FL, USA, November 28 - December 1, 2022, pp. 1245–1250.
 - [20] Y. Cui, K. Cao, G. Cao, M. Qiu, and T. Wei, “Client scheduling and resource management for efficient training in heterogeneous IoT-edge federated learning,” *IEEE Trans. Comput. Aided Des. Integr. Circuits Syst.*, vol. 41, no. 8, pp. 2407–2420, 2022.
 - [21] W. Gao, Z. Zhao, G. Min, Q. Ni, and Y. Jiang, “Resource allocation for latency-aware federated learning in industrial internet of things,” *IEEE Trans. Ind. Informatics*, vol. 17, no. 12, pp. 8505–8513, 2021.
 - [22] D. Jhunjhunwala, A. Gadhikar, G. Joshi, and Y. C. Eldar, “Adaptive quantization of model updates for communication-efficient federated learning,” in *Proceedings of the IEEE International Conference on Acoustics, Speech and Signal Processing*, Toronto, ON, Canada, June 6–11, 2021, pp. 3110–3114.
 - [23] Z. Jiang, Y. Xu, H. Xu, Z. Wang, J. Liu, Q. Chen, and C. Qiao, “Computation and communication efficient federated learning with adaptive model pruning,” *IEEE Trans. on Mobile Comput.*, pp. 1–18, 2023.
 - [24] R. Hu, Y. Gong, and Y. Guo, “Federated learning with sparsification-amplified privacy and adaptive optimization,” in *Proceedings of the Thirtieth International Joint Conference on Artificial Intelligence*, Virtual Event / Montreal, Canada, August 19–27, 2021, pp. 1463–1469.
 - [25] Z. Tang, S. Shi, B. Li, and X. Chu, “GossipFL: A decentralized federated learning framework with sparsified and adaptive communication,” *IEEE Trans. Parallel Distributed Syst.*, vol. 34, no. 3, pp. 909–922, 2023.
 - [26] H. Sun, X. Ma, and R. Q. Hu, “Adaptive federated learning with gradient compression in uplink NOMA,” *IEEE Trans. Veh. Technol.*, vol. 69, no. 12, pp. 16 325–16 329, 2020.
 - [27] C. Chen, L. Shen, H. Huang, and W. Liu, “Quantized Adam with error feedback,” *ACM Trans. Intell. Syst. Technol.*, vol. 12, no. 5, pp. 56:1–56:26, 2021.
 - [28] C. Chen, L. Shen, W. Liu, and Z. Luo, “Efficient-Adam: Communication-efficient distributed Adam with complexity analysis,” *CoRR*, vol. abs/2205.14473, 2022.
 - [29] H. Tang, S. Gan, A. A. Awan, S. Rajbhandari, C. Li, X. Lian, J. Liu, C. Zhang, and Y. He, “1-bit Adam: Communication efficient large-scale training with Adam’s convergence speed,” in *Proceedings of the 38th International Conference on Machine Learning*, vol. 139, Virtual Event, July 18–24, 2021, pp. 10 118–10 129.
 - [30] J. Mills, J. Hu, and G. Min, “Communication-efficient federated learning for wireless edge intelligence in iot,” *IEEE Internet Things J.*, vol. 7, no. 7, pp. 5986–5994, 2020.
 - [31] S. U. Stich, J. Cordonnier, and M. Jaggi, “Sparsified SGD with memory,” in *Advances in Neural Information Processing Systems 31*, Montréal, Canada, December 3–8, 2018, pp. 4452–4463.
 - [32] P. Prakash, J. Ding, R. Chen, X. Qin, M. Shu, Q. Cui, Y. Guo, and M. Pan, “Iot device friendly and communication-efficient federated learning via joint model pruning and quantization,” *IEEE Internet Things J.*, vol. 9, no. 15, pp. 13 638–13 650, 2022.
 - [33] Y. Li, W. Li, B. Zhang, and J. Du, “Federated Adam-type algorithm for distributed optimization with lazy strategy,” *IEEE Internet Things J.*, vol. 9, no. 20, pp. 20 519–20 531, 2022.
 - [34] S. Bock and M. G. Weiß, “Non-convergence and limit cycles in the Adam optimizer,” in *Artificial Neural Networks and Machine Learning - ICANN 2019: Deep Learning*, vol. 11728, Munich, Germany, September 17–19, 2019, pp. 232–243.
 - [35] Z. Liu, Z. Shen, S. Li, K. Helweggen, D. Huang, and K. Cheng, “How do Adam and training strategies help bnns optimization,” in *Proceedings of the 38th International Conference on Machine Learning*, vol. 139, Virtual Event, July 18–24, 2021, pp. 6936–6946.
 - [36] M. Yurochkin, M. Agarwal, S. Ghosh, K. H. Greenewald, T. N. Hoang, and Y. Khazaeni, “Bayesian nonparametric federated learning of neural networks,” in *Proceedings of the 36th International Conference on Machine Learning*, vol. 97, Long Beach, California, USA, June 9–15, 2019, pp. 7252–7261.
 - [37] H. Wang, M. Yurochkin, Y. Sun, D. S. Papailiopoulos, and Y. Khazaeni, “Federated learning with matched averaging,” in *Proceedings of the 8th International Conference on Learning Representations*, Addis Ababa, Ethiopia, April 26–30, 2020.
 - [38] E. Ozfatura, K. Ozfatura, and D. Gündüz, “Time-correlated sparsification for communication-efficient federated learning,” in *Proceedings of IEEE International Symposium on Information Theory, Melbourne, Australia, July 12–20, 2021*, pp. 461–466.
 - [39] X. Lin, Y. Liu, F. Chen, X. Ge, and Y. Huang, “Joint gradient sparsification and device scheduling for federated learning,” *IEEE Trans. Green Commun. Netw.*, vol. 7, no. 3, pp. 1407–1419, 2023.
 - [40] P. Han, S. Wang, and K. K. Leung, “Adaptive gradient sparsification for efficient federated learning: An online learning approach,” in *Proceedings of the 40th IEEE International Conference on Distributed Computing Systems*, Singapore, November 29 - December 1, 2020, pp. 300–310.

This figure "fig1.png" is available in "png" format from:

<http://arxiv.org/ps/2405.17932v1>